International Food Research Journal 31(3): 737 - 747 (June 2024)
Journal homepage: *http://www.ifrj.upm.edu.my*

Development and characterisation of agar/silver nanoparticles-based film from *Gracilaria canaliculata* for food packaging

Preethi, B. and *Vijaya Geetha, B.

Department of Biotechnology, Rajalakshmi Engineering College, Thandalam, Chennai, India

Article history

Received:
8 October 2023
Received in revised form:
6 April 2024
Accepted:
14 April 2024

Keywords

Gracilaria canaliculata,
silver nanoparticles,
agar,
food packaging,
film

Abstract

Gracilaria canaliculata was used as a novel source to extract agar, and for the green synthesis of silver nanoparticles. Silver nanoparticles (0.1 - 0.3%) were incorporated into the agar matrix to develop an environment-friendly food packaging material using the solution casting method. The concentration of nanoparticles affected the physical, thermal, and mechanical properties of the films. Films containing higher concentrations of silver nanoparticles exhibited promising properties, and demonstrated strong antimicrobial activity against both Gram-negative and Gram-positive foodborne pathogens. The film formulation exhibited no cytotoxic effect on HepG2 cells, with cell viability exceeding 94%. These findings suggested that the film possessed favourable characteristics for use as a food packaging material, presenting a potential alternative to plastics.

DOI
https://doi.org/10.47836/ifrj.31.3.17

Introduction

The use of plastic for food packaging has grown dramatically due to its favourable physicochemical properties and low cost. However, this has led to excessive waste generation and accumulation because plastics are highly resistant to biodegradation (Basumatary *et al*., 2018). Consumers are increasingly demanding for eco-friendly food packaging options (Cazon *et al*., 2017). This trend has driven the development of biodegradable packaging materials from renewable sources like biopolymers (Ekrami and Emam-Djomeh, 2014). These biopolymers offer advantages beyond biodegradability, including biocompatibility, edibility, and resistance to oxygen and physical pressure (Handayasari *et al*., 2019).

Numerous studies have explored food packaging materials derived from biopolymers like carbohydrates, proteins, and lipids. Carbohydrates are considered particularly promising due to their film-forming ability and adequate mechanical and barrier properties (Malgurski *et al*., 2017). Among carbohydrates, agar extracted from seaweed is commonly used for developing packaging materials (Kumar *et al*., 2019). Agar is composed of the polysaccharide agarose and agaropectin, with agarose contributing to its gelling properties (Martinez-Sanz *et al*., 2019). Additionally, agar can form transparent, stretchable, and flexible films when maintained at a lower pH (Roy and Rhim, 2019a). Agar is also economical, biodegradable, and safe for use, making it a potential substitute for synthetic plastics (Huang *et al*., 2020). Despite its advantages, agar-based packaging has a major limitation: poor resistance to microbial growth. This renders it incapable of preventing food spoilage caused by microorganisms, which negatively impacts food quality (Handayasari *et al*., 2019). Furthermore, due to its hydrophilic nature, agar-based packaging films exhibit weak mechanical properties, and act as poor barriers to water vapour.

To address these limitations and enhance the film's antimicrobial and mechanical properties, nanoparticles and nanoclays are being incorporated (Roy and Rhim, 2019b). Among these nanomaterials, silver nanoparticles (AG NP) have proven to be particularly effective antimicrobial agents (Kumar *et al*., 2017). They possess broad-spectrum antimicrobial activity, and their efficacy in packaging

*Corresponding author.
Email: vijayageetha.b@rajalakshmi.edu.in

films depends on factors such as particle size, silver concentration, and interaction with the polymeric matrix (Rhim *et al*., 2014). The high surface area to volume ratio of AG NP allows for better interaction with microorganisms (Ghosh *et al*., 2010). Traditionally, AG NP are synthesised by reducing silver ions from silver salts. However, for the development of non-toxic and eco-friendly AG NP-biopolymer based packaging films, green synthesis methods are preferred, which utilise plant materials-containing agents such as polyphenols and alkaloids, which act as reducing and stabilising agents (Roopan *et al*., 2013).

Therefore, the main objectives of the present work were to extract agar by native method, synthesise AG NP from *Gracilaria canaliculata*, and develop agar-based nanocomposite films by incorporating AG NP for food packaging applications. The prepared agar-based AG NP-containing film was subjected for evaluation for its physical, mechanical, thermal, and antimicrobial properties.

Materials and methods

Seaweed

Gracilaria canaliculata was obtained from the Kamuti cultivation site, Rameswaram, Ramanathapuram District, Tamil Nadu, India. Harvested algae were dried under shade, cleaned, and stored in moisture-free containers.

Chemicals used were silver nitrate and polyethylene glycol, purchased from Nice Chemicals, India; and sodium borohydride and glycerol, purchased from SRL, India.

Methodology

Agar extraction from G. canaliculata

Dried algae, obtained through pen culture (100 g), were taken and washed with water to eliminate sand, salt, and other debris. The cleaned algae were soaked in 500 mL of distilled water for 24 h, and kept in a water bath at 90°C for 1.5 h. The soaked algae were ground to a fine paste using 500 mL of distilled water in an electrical homogeniser. The slurry was then kept in a tight container, and placed in an autoclave for 3 h at 121°C and 15 lb pressure for complete extraction of agar from the algae. The autoclaved sample was filtered using muslin cloth (mesh size 120), and the filtrate was kept in a freezer at -10°C overnight. The sample was then thawed to remove excess water. The extracted sample was dried at 70°C for 3 h. The dried sample was powdered using a homogeniser, and the yield was recorded.

Synthesis of AG NP from G. canaliculata

The cleaned algal powder was heated at 90°C for 45 min in deionised water (Kumar *et al*., 2013). A 0.5% extract was prepared. To 10 mL of this extract, 10 mL of 1 mM $AgNO_3$ was added. This solution was left in a stirrer at 75°C for 15 min, followed by ultrasonication in a bath-sonicator. The mixture was then centrifuged at 3,000 rpm for 30 min. The supernatant collected after the centrifugation process was assessed using UV spectrophotometer.

Agar-AG NP-containing film formulation and development

Ten grams of extracted agar were added to 100 mL pre-heated (70°C) distilled water while continuously stirring on a magnetic stirrer. After stirring for 10 min at 1,000 rpm, 5 g polyethylene glycol was slowly added. This solution was kept in a water bath at 95°C for 1 h to provide uniform consistency to the film solution. To this hot solution, 5 mL of glycerol was added dropwise while stirring at 1,500 rpm. The solution was cooled down to 40 - 50°C in ambient conditions. After cooling, three different concentrations of freshly prepared AG NP were added. The concentration of the added AG NP was maintained at 0.1, 0.2, and 0.3% for 100 mL film solution prepared. The solution casting method (Roy and Rhim, 2019b) was followed to obtain agar-AG NP-containing films. The films were cast on sterilised (121°C, 15 lb pressure) glass Petri plates. To 150 mm glass plates, 10 mL of film solution was slowly added to avoid air bubble formation. The plates were left in a covered chamber overnight for the films to form at room temperature. The films were peeled off from the plates, and stored in sterile packs for further analysis.

Characterisation of agar-AG NP-containing film

Moisture content measurement

The moisture content of the samples was measured using a moisture balance (Shimadzu-Unibloc MOC63u) based on the loss on drying method. The instrument was pre-set to a temperature of 120°C, and a 1 × 1 cm film was placed on the sample tray for estimation. Eq. 1 was used for estimation:

$$\text{Moisture content (\%)} = \frac{Initial\ weight - Final\ weight}{Initial\ weight} * 100 \quad \text{(Eq. 1)}$$

Thickness

The thicknesses of the films were measured using a digital micrometre with an accuracy of 0.001 mm.

Swelling ratio determination

The method described by Roy and Rhim (2019a) was adopted with minor modifications. The film samples were cut to 1 × 1 cm size, weighed, and recorded as initial weight (IW). The samples were then placed in a beaker containing 10 mL of distilled water for 24 h. After 24 h of soaking, the excess water was removed using blotting paper, and the weight of the samples was recorded again as final weight (FW). The swelling ratio was then determined using Eq. 2:

$$\text{Swelling ratio (\%)} = \frac{FW - IW}{IW} * 100 \quad \text{(Eq. 2)}$$

Water vapour permeability estimation

The standard gravimetric method ASTM E96/E96M-22 (ASTM, 2022) was applied. A temperature of 25°C and 50% RH were maintained throughout the process, and water vapour transmission measuring cups were used for the test. The WVP was calculated using Eq. 3:

$$WV_p(\text{g m/m}^2\text{sPa}) = \frac{(WVTR * L)}{\Delta P} \quad \text{(Eq. 3)}$$

where, WVTR (g/m^2s) = water vapour transmission rate obtained from the experiment, ΔP (Pa) = partial vapour pressure from one side of the film to another, and L (m) = mean thickness of the film.

UV-Vis spectrophotometric analysis

Hitachi UH5300 UV-Vis spectrophotometer was used to conduct the UV-Vis spectrophotometric analysis of the synthesised AG NP and the three film formulations, including control, 0.1, 0.2, and 0.3% AG NP incorporated films.

FTIR analysis

FTIR analysis was carried out in the range of 4000 - 400 cm^{-1} for the control and test samples using a Cary 600 series (ATR), Agilent Technologies.

Testing of mechanical properties

A Universal Testing Machine, TKG-/TKG-EC with a measuring range of 0 - 200 N, and an elongation speed of 1 mm, with a vive-type grip was used to hold the films in position. It was used to determine the tensile strength (TS) and the elongation at break (E) of the films. The grip separation was set to 50 mm, and the traverse speed was adjusted to 50 mm/min. All film samples were cut to 3 × 10 mm size. The procedure was conducted according to ASTM D882-18 (ASTM, 2018) standards for thin sheets and films.

Thermal stability

Thermogravimetric analysis and differential scanning calorimetry were performed to determine the thermal properties for the control and test samples. Ten micrograms of the sample were used for analysis in the thermogravimetric analyser (Netzsch-STA 2500 Regulus). The TA Instruments DSC25 was used for differential scanning calorimetry test (Shukla *et al*., 2012) in the temperature range of 0 - 550°C. A broad temperature range was used as the films might be exposed to harsh temperature conditions in real-time in the food packaging industries.

Scanning electron microscopy of the developed film

The microstructure of the agar films was examined using a scanning electron microscope (SEM; Thermoscientific Apreo S), a standard HR-SEM instrument.

Antimicrobial activity studies

The agar plating method was employed to determine the antimicrobial activity of the agar/AG NP-containing films. The procedure outlined by Shukla *et al*. (2012) was adopted with slight alterations. Agar plates were prepared following a standardised protocol. The prepared agar-AG NP-containing films were cut into 4 mm discs, washed, and vacuum-dried for 1 h prior to antimicrobial activity testing. Two major foodborne pathogens, *Escherichia coli* and *Staphylococcus aureus*, were used for this purpose. Bacterial suspension was spread-plated on the previously prepared agar plates. The control film (without NP), 0.1, 0.2, and 0.3% agar-AG NP-containing films were placed on the agar plates accordingly. The plates were sealed and incubated for 24 h at 37°C. The zones of inhibition by the films were recorded after the 24-h period.

Determination of cytotoxic effect and cell viability

An MTT assay kit (Millipore, USA) was utilised to determine the cytotoxic effect, cell viability, and proliferation on HepG2 cells. For culturing, 96-well plates containing 100 µL of HepG2 cells and Dulbecco's modified Eagle Medium (DMEM) were used. The medium was further enriched with 100 IU/mL penicillin and 10% foetal bovine serum. The plates were then placed in a CO_2 incubator at 37°C for 24 h. Test film formulations were added to the wells in triplicates. After 24 h of incubation, the media was replaced with 10 µL of MTT solution (5 mg/m in PBS) in 100 µL of freshly prepared media. This was followed by 4 h of incubation of the plates. The formed formazan crystals in the well plates were dissolved in 0.1 mL DMSO (Sarwar *et al*., 2018). The dissolved MTT formazan crystals' optical density was finally measured using an ELISA plate reader at 570 and 620 nm for test and reference wavelengths, respectively. The cell viability was estimated using Eq. 4:

$$\text{Percent cell viability} = \frac{Test\ 570\ nm-620\ nm}{Control\ 570\ nm-620\ nm} * 100 \quad \text{(Eq. 4)}$$

Statistical analysis

All the experiments (Table 1) were done in triplicates, and the observed results were analysed using Graphpad software. Student's *t*-test was used to evaluate the significant difference between control and test films. The results were represented as mean ± SD. A $p < 0.05$ were considered to be significant.

Table 1. Physical/mechanical characterisation (moisture, thickness, swelling, water vapour permeability, tensile strength, and elasticity) and antimicrobial activity (zone of inhibition) of developed films.

Parameter / Film	Control	Agar - 0.1% AG NP	Agar - 0.2% AG NP	Agar - 0.3% AG NP
Moisture content (%)	11.19 ± 0.001	11.15 ± 0.0005	11.14 ± 0.001	11.14 ± 0.0005
Thickness (mm)	0.081 ± 0.001	0.072 ± 0.0005	0.071 ± 0	0.071 ± 0.005
Swelling ratio (%)	14.42 ± 0.005	14.41 ± 0.01	14.07 ± 0.058	12.32 ± 0.015
Water vapour permeability ($*10^{-10}$ g m/m^{2}sPa)	0.157 ± 0.001	0.152 ± 0.001	0.146 ± 0.001	0.147 ± 0.001
Tensile strength (MPa)	31.02 ± 0.011	32.52 ± 0.015	32.55 ± 0.015	32.59 ± 0.015
Elongation at break (%)	24.03 ± 0.015	25.53 ± 0.010	25.94 ± 0.011	25.95 ± 0.011
Zone of Inhibition for *E. coli* (mm)	0.00	5.00 ± 1.00	7.67 ± 0.58	7.67 ± 0.58
Zone of Inhibition for *S. aureus* (mm)	0.00	4.6 ± 0.58	6.66 ± 0.5	7.00 ± 1.00

Control: film formulation without AG NP; Agar - 0.1% AG NP: 0.1% AG NP/100 mL film formulation; Agar - 0.2% AG NP = 0.2% AG NP/100 mL film formulation; Agar - 0.3% AG NP: 0.3% AG NP/100 mL film. Values are mean ± SD of triplicates, and the results are significant with $p < 0.05$.

Results and discussion

From 100 g of dried algae, 28 g of agar yield was obtained, and the final AG NP obtained exhibited a golden yellow colour, which was confirmed through UV-spectrophotometric analysis.

Physical characterisation of the film

The physical characteristics of the control and test samples (Figure 1a) are summarised in Table 1. The moisture content of the control and test films ranged from 11.14 to 11.19%. The presence of moisture could have been due to the water-sensitive characteristics of algal agar (Omerovic *et al*., 2021). From the moisture values obtained, it was inferred that the addition of nanoparticles or increasing their concentration did not have a remarkable impact on the moisture content of the films. This inference agreed with Roy *et al*. (2019) when copper nanoparticles were added to agar films. Regarding the swelling ability results, the swelling ratio of the control film was higher. This could have been due to the presence of agar, a hydrophilic polymer with a greater ability to attract water. In AG NP-containing

films, the swelling ratio was lower than that in control films, as AG NP contributed to some degree of crosslinking in the films, reducing gaps in the polymer matrix, and providing resistance to the entry of water molecules (Ediyilyam *et al*., 2021). The swelling ratio decreased with increasing concentration of AG NP. The water vapour permeability of the control film was higher than that of the test films. As the concentration of AG NP increased, the water vapour permeability rate decreased. The rate of water vapour permeation might have been influenced by the presence of glycerol (Ekrami and Emam-Djomeh, 2014), although the major decrease in water vapour movement into the film could have been due to the presence of AG NP (Rhim *et al*., 2013). The decrease in water permeation might have occurred due to increased crystallinity resulting from nanoparticle addition, and the strong interaction of nanoparticles with the polymeric agar, thus forming a superior barrier (Jafarzadeh and Jafari, 2021). Resistance to water is crucial for preventing microbial degradation of food, and a factor in evaluating the stability of packaging films (Maisanaba *et al*., 2019).

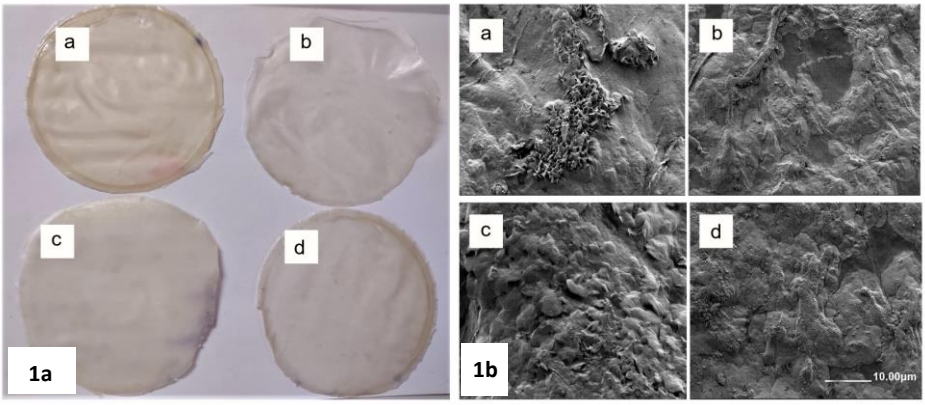

Figure 1. (1a) Image of control and developed test films. **(1b)** SEM images of control and developed test films. **(a)** Control: film formulation without AG NP; **(b)** Agar - 0.1% AG NP: 0.1% AG NP/100 mL film formulation; (c) Agar - 0.2% AG NP: 0.2% AG NP/100 mL film formulation; and **(d)** Agar - 0.3% AG NP: 0.3% AG NP/100 mL film formulation.

UV-Vis spectrophotometric analysis

UV-Vis spectrophotometric analysis was conducted for the synthesised AG NP and the formulated film solutions. The results are illustrated in Figure 2. The spectrum of the nanoparticle exhibited a peak in the range of 280 - 310 nm, which is characteristic of AG NP. The peaks for the control and test films for agar-nanoparticle films were observed in the range of 400 - 430 nm (Shankar and Rhim, 2015).

Fourier transform infrared (FTIR) spectroscopic analysis

FTIR analysis was performed for both control and test films (Figure 3). The similarity in the results of all three test films indicated notable strong bonding formed between the major film component agar and AG NP. In all cases, a broad range peak at 3420 - 3300 cm^{-1} denotes the O-H stretching of the hydroxyl group, indicating the presence of a polymer compound, in this case, agar being the major contributor. The peak observed in the range of 1637 cm^{-1} was distinct and due to the presence of an NH group along with CO stretching in the agar. The peak around 1372 cm^{-1} represents the sulphate ester present in the polysaccharide agar, and the β-galactose peak was observed around 1334 cm^{-1} (Shankar *et al*., 2015b). The range of 930 - 1070 cm^{-1} denotes peaks for the presence of 3,6-anhydrogalactose in the extracted agar used in the film formulation (Rhim *et al*., 2014).

Mechanical properties (thickness, elongation, and tensile strength)

The mechanical properties of the films depended thoroughly on the formulation. The thicknesses of the films were less than 1 mm in all cases. The addition of nanoparticles did not affect the thickness of the films, confirming that the nanoparticles are equally distributed, and in favourable sizes. In a similar study, 1-mm films were obtained when AG NP were added (Shankar and Rhim, 2015). Plasticisers were added to the films to positively alter their mechanical characteristics. In the

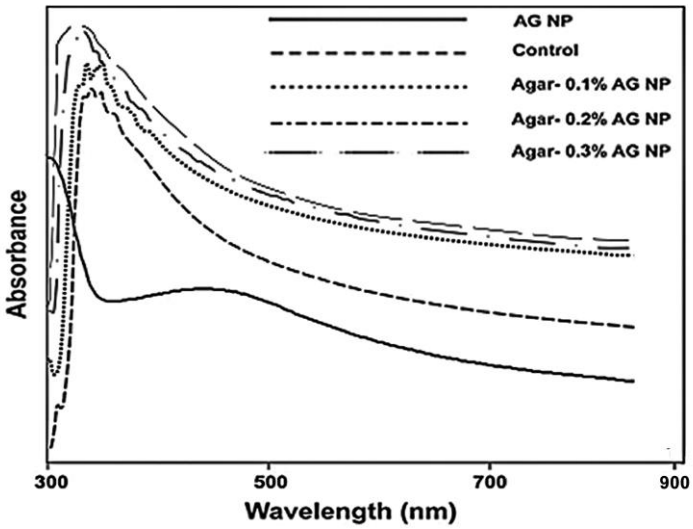

Figure 2. UV-Vis spectrum of synthesised AG NP from *Gracilaria canaliculata*, control film formulation, and test film formulations. Control: film formulation without AG NP; Agar - 0.1% AG NP: 0.1% AG NP/100 mL film formulation; Agar - 0.2% AG NP: 0.2% AG NP/100 mL film formulation; Agar - 0.3% AG NP: 0.3% AG NP/100 mL film formulation; and nm: nanometre.

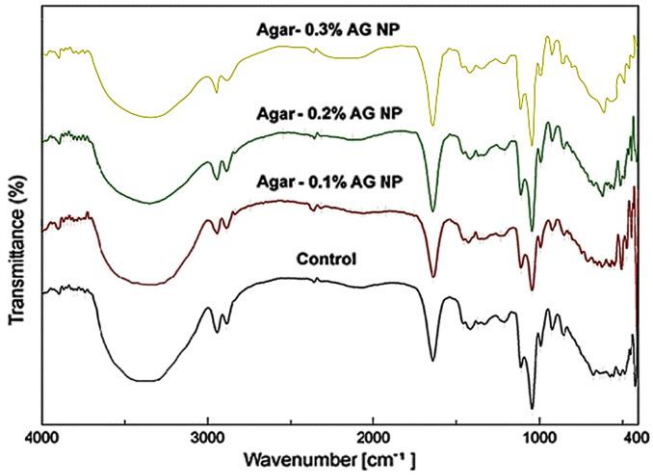

Figure 3. Fourier transform infrared spectroscopic analysis of control, Agar - 0.1% AG NP, and Agar - 0.2% AG NP films. Control: film formulation without AG NP; Agar - 0.1% AG NP: 0.1% AG NP/100 mL film formulation; Agar - 0.2% AG NP: 0.2% AG NP/100 mL film formulation; Agar - 0.3% AG NP: 0.3% AG NP/100 mL film formulation; and cm^{-1}: centimetre inverse.

present work, glycerol and polyethylene glycol were added, enhancing the properties of the films (Taherimehr *et al*., 2021), and significantly improving their elastic nature, providing favourable flexibility. The elasticity of the film is crucial in the food packaging industries. The nanoparticle-containing films displayed a notable increase in tensile strength and elongation compared with control films. The elongation was favourable, ranging from 25 to 26% (Table 1) for the test films. Good blending between the AG NP and the plasticisers glycerol and polyethylene glycol, along with the polymeric properties of agar, largely contributed to this property. The values for elongation (%) of the films were well substantiated with the results derived when chitosan was used along with agar to develop composite films (Huang *et al*., 2020), where chitosan improved the flexible nature of the film. Regarding tensile strength, the tensile strength of all the test films ranged from 31 - 32.55% and the highest was recorded for 0.3% AG NP film. The addition of AG NP reinforced the agar with mechanical strength, possibly due to strong intermolecular bonding between agar and AG NP, supporting enhanced

load/stress transfer (Shankar and Rhim, 2017; Dungani *et al*., 2021).

Thermal stability testing

TGA analysis provided details on the thermal decomposition of the film on a weight basis. TGA results revealed that the thermal loss of the film started in the temperature range of 95 - 100°C in the first stage, possibly due to the loss of water and the solvent used during film preparation (Rhim *et al.*, 2013). Decomposition of water continued beyond 100°C due to the presence of hydrogen bonds (El-Hefian *et al*., 2012). The second level of decomposition started at around the temperature of 250 - 310°C, which might have been caused by the plasticiser glycerol (Basumatary *et al*., 2018), followed by intense material loss at very high temperatures (El-Hefian *et al*., 2012). The intense loss might have occurred due to the thermal decomposition of organic groups present in the agar (Basumatary *et al*., 2018). Similar results have been reported in an earlier study conducted by Shankar *et al*. (2015a) on agar-based films. The onset temperature of thermal decomposition of the film containing 0.3% AG NP was slightly higher than that of the control (Kumar *et al*., 2019), indicating the subtle impact of AG NP on the thermal characteristics of the film. Figure 4a depicts the thermal stability of the control and test sample films. From the DSC thermogram (Figure 4b) obtained, the onset temperature of all the test samples fell in the range of 98 - 113°C. The exothermic peaks of the samples representing the crystallisation temperature were observed at around 76 - 80°C for both the control and test samples. Furthermore, endothermic peaks were also observed. For the control, the onset temperature was about 262°C, and the endothermic peak occurred at around 270°C. Similarly, for AG NP-containing agar films, the onset temperatures were about 160 - 170°C, and the endothermic peaks fell in the range of about 178 - 190°C.

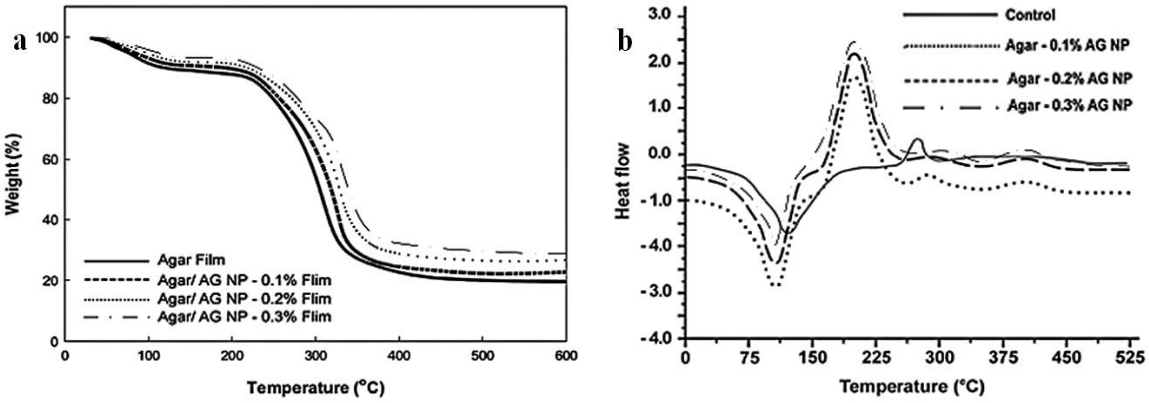

Figure 4. (a) Thermal stability testing of control and developed test films. **(b)** Differential scanning calorimetry of control and developed test films. Control: film formulation without AG NP; Agar - 0.1% AG NP: 0.1% AG NP/100 mL film formulation; Agar - 0.2% AG NP: 0.2% AG NP/100 mL film formulation; Agar - 0.3% AG NP: 0.3% AG NP/100 mL film formulation; and °C: degree Celsius.

SEM images of the test films

SEM analysis (Figure 1b) of the control and test films was conducted to understand the microscopic structure and morphology of the film surface. Agar and AG NP were observed to blend well. The uniform distribution of nanoparticles in the agar matrix could have been due to its roughness, as studies have shown that the addition of AG NP would result in a rough surface due to the coexisting protruded film structure. Additionally, there were no notable agglomerations observed, which might reduce nanoparticle-matrix contact (Dungani *et al*., 2021). The lack of agglomeration would improve mechanical strength, as evident from the results obtained in relation to the control films (Jafarzadeh and Jafari, 2021). The ridge-like structure seen added to the ductility of the film (Hernandez-Izquierdo and Krochta, 2008).

Antimicrobial activity studies

The zone of inhibition values clearly indicated the antimicrobial activity of the AG NP. The control films consisting only of agar and plasticisers did not exhibit any clear zones of inhibition, which could have been due to the lack of antimicrobial activity of the film (Malgurski *et al*., 2017). In the case of AG

NP-added films, clear zones of inhibition were visualised against *E. coli* and *S. aureus*, consistent with earlier studies (Taherimehr *et al*., 2021). The zone of inhibition increased with the increase in the concentration of AG NP from 0.1 to 0.2%, although no drastic increase was recorded between 0.2 and 0.3% AG NP-containing films, similar to previous research (Ghosh *et al*., 2010). Nanoparticles are advantageous over plant-based antimicrobial substances, as the latter show activity more prominently only in Gram-positive bacteria (Heydari *et al*., 2020; Noshad *et al*., 2021), since the outer cell wall of Gram-negative bacteria is composed of lipopolysaccharide barriers (Sureshjani *et al*., 2014), which are difficult to penetrate. In the present work, the zone of inhibition was recorded higher for *E. coli*, showing clear control of AG NP on the multiplication of Gram-negative bacteria. The zones of inhibition of the control and test samples against *E. coli* and *S. aureus* are presented in Table 1. In both cases, AG NP could have played a role in restricting the replication of pathogens by penetrating the cell membrane and generating reactive oxygen species, imparting an overall bactericidal activity.

Determination of cytotoxic effect and cell viability

Human hepatocytes are used as primary models to investigate xenobiotic cytotoxicity (Guillouzo *et al*., 2007). Cell lines have replaced the usage of fresh liver cell samples due to limitations such as low lifespan and difficult isolation protocols (Madan *et al*., 2003). Consequently, HepG2 cell lines are used in the present work to determine the cytotoxic effect of film formulations, as they have been previously used in such experiments. MTT would be converted to formazan crystals by the enzyme succinic dehydrogenase in the mitochondria of living cells (Mosman, 1983), and viable cell count was estimated through this process. Different concentrations (50, 100, 150, 200, 250 µg/mL) of 0.1 - 0.3% test film formulations were studied, and an AG NP-free formulation was used as control. From the MTT assay results, it could be inferred that the control film solution displayed 100% viability, whereas cells exposed to 0.1, 0.2, and 0.3% AG NP-containing formulations displayed cell viabilities of 97, 95, and 94%, respectively, even at the highest concentration of 250 µg/mL. Since the viability was > 90%, the film formulations were proven to be non-toxic to HepG2 cells. Previous research results have shown that viability of > 75% would be considered non-toxic. For instance, a cell viability of 97.8% was obtained when L929 cell lines were exposed to polyurethane/chitosan/nano ZnO composite films (Maisanaba *et al*., 2019), and low toxicity was observed in studies conducted using starch-capped AG NP. In another study, PVA films with nanocellulose and starch-capped AG NP did not show a toxic effect on hepatocytes (Omerovic *et al*., 2021), and similar experiments by Hajji *et al*. (2017) also proved that chitosan-PVA AG NP-containing films had no toxic effect on CHO-K1 cell lines, with resultant viability reported to be > 70%. Additionally, the lowered cytotoxicity reported here, and resultant cell viability could have been due to the polymeric matrix that would aid in the controlled release of nanoparticles. In accordance with previous research, it is safe to suggest that low concentrations of AG NP (0.1 - 0.3%) added to 100 mL film formulation did not exhibit any cytotoxic effect on HepG2 cell lines, hence were safe at the studied concentrations.

Conclusion

An environmentally friendly food packaging material was developed using agar and AG NP obtained from *G. canaliculata*. The developed film was characterised based on physical, mechanical, thermal, and antimicrobial properties. Films with a thickness of < 1 mm were obtained. FTIR and SEM analysis showed that the AG NP dispersed uniformly in the agar matrix. The addition of AG NP decreased the swelling ratio, prevented water vapour permeability, and considerably increased tensile strength. All these results could have be due to the strong interaction between agar and AG NP, making the film crystalline, thereby acting as a good barrier. Additionally, the combination of agar, glycerol, polyethylene glycol, and AG NP improved the elongation and flexibility of the film. AG NP-incorporated films exhibited strong antimicrobial activity against both Gram-positive and Gram-negative bacteria. Furthermore, the cytotoxic effect of AG NP-containing film on HepG2 cells was studied, and resultant cell viability was estimated to be > 94%. The favourable barrier properties, mechanical strength, along with antimicrobial and non-toxic nature, make *G. canaliculata* agar-based food packaging material suitable for commercial food packaging.

References

American Society for Testing and Materials (ASTM). 2018. D882-18 - Standard test method for tensile properties of thin plastic sheeting. United States: ASTM.

American Society for Testing and Materials (ASTM). 2022. ASTME96/E96M-22 - Standard test methods for gravimetric determination of water vapour transmission rate of materials. United States: ASTM.

Basumatary, K., Daimary, P., Das, S. K., Thapa, M., Singh, M., Mukherjee, A. and Kumar, S. 2018. *Lagestroemia speciose* fruit-mediated synthesis of silver nanoparticles and its application as filler in agar based nanocomposite films for antimicrobial food packaging. Food Packaging and Shelf Life 17: 99-106.

Cazon, P., Velazquez, G., Ramirez-De-Leon, J. A. and Vazquez, M. 2017. Polysaccharide-based films and coatings for food packaging: A review. Food Hydrocolloids 68: 136-148.

Dungani, R., Sumardi, I., Suhaya, Y., Aditiawati, P., Dody, S., Rosamah, E., ... and Karliati, T. 2021. Reinforcing effects of seaweed nanoparticles in agar-based biopolymer composite: Physical, water vapour barrier, mechanical and biodegradable properties. BioResources 16(3): 5118-5132.

Ediyilyam, S., George, B., Shankar, S. S., Dennis, T. T., Waclawek, S., Cernik, M. and Padil, V. T. 2021. Chitosan/gelatin/silver nanoparticles composite films for biodegradable food packaging applications. Polymers 13(11): 1-18.

Ekrami, M. and Emam-Djomeh, Z. 2014. Water vapour permeability, optical and mechanical properties of salep-based edible film. Journal of Food Processing and Preservation 38(4): 1812-1820.

El-Hefian, E. A., Nasef, M. M. and Yahaya, A. H. 2012. Preparation and characterization of chitosan/agar blended films: Part 2 - Thermal, mechanical and surface properties. Journal of Chemistry 9: 510-516.

Ghosh, S., Kaushik, R., Nagalakshmi, K., Hoti, S. L., Menzes, G. A., Harish, B. N. and Vasan, H. N. 2010. Anti-microbial activity of highly stable silver nanoparticles embedded in agar-agar matrix as a thin film. Carbohydrate Research 345: 2220-2227.

Guillouzo, A., Corlu, A., Aninat, C., Glasier, D., Morel, F. and Guguen-Guillouzo, C. 2007. The human hepatoma HepaRG cells: A highly differentiated model for studies of liver metabolism and toxicity in xenobiotic. Chemico-Biological Interactions 168(1): 66-73.

Hajji, S., Salem, R. B. S. B., Hamdi, M., Jellouli, K., Ayadi, W., Nasrin, M. and Boufi, S. 2017. Nanocomposite films based on chitosan-poly (vinyl alcohol) and silver nanoparticles with high antibacterial and antioxidant activities. Process Safety and Environmental Protection 111: 112-121.

Handayasari, F., Suyatma, N. E. and Nurjanah, S. U. 2019. Physicochemical and antibacterial analysis of gelatin-chitosan edible film with the addition of nitrite and garlic essential oil by response surface methodology. Journal of Food Processing and Preservation 43(12): 1-10.

Hernandez-Izquierdo, V. M. and Krochta, J. M. 2008. Thermoplastic processing of proteins for film formation - A review. Journal of Food Science 73(2): 30-39.

Heydari, S., Jooyandeh, H., Behbahani, B. A. and Noshad, M. 2020. The impact of Qodume Shirazi seed mucilage-based edible coating containing lavender essential oil on the quality enhancement and shelf life improvement of fresh ostrich meat: An experimental and modeling study. Food Science and Nutrition 8(12): 6497-6512.

Huang, D., Zhang, Z., Zheng, Y., Quan, Q., Wang, W. and Wang, A. 2020. Synergistic effect of chitosan and halloysite nanotubes on improving agar film properties. Food Hydrocolloids 101: 105471.

Jafarzadeh, S. and Jafari, S. M. 2021. Impact of metal nanoparticles on the mechanical, barrier, optical and thermal properties of biodegradable food packaging materials. Critical Reviews in Food Science 61(16): 2640-2658.

Kumar, P., Senthamil Selvi, S. and Govindraju, M. 2013. Seaweed-mediated biosynthesis of silver nanoparticles using *Gracilaria corticata* for its antifungal activity against *Candida* spp. Applied Nanoscience 3: 495-500.

Kumar, S., Boro, J. C., Ray, D., Mukherjee, A. and Dutta, J. 2019. Bionanocomposite films of agar incorporated with ZnO nanoparticles as an active packaging material for shelf life extension of green grape. Heliyon 5(6): 1-8.

Kumar, S., Mitra, A. and Halder, D. 2017. *Centella asiatica* leaf mediated synthesis of silver nanocolloid and its application as filler in gelatin based antimicrobial nanocomposite film. LWT - Food Science and Technology 75: 293-300.

Madan, A., Graham, R. A., Carroll, K. M., Mudra, D. R., Burton, L. A. and Ribadeneria, M. D. 2003. Effects of prototypical microsomal enzyme inducers on cytochrome P450 expression in cultured human hepatocytes. Drug Metabolism and Disposition 31(4): 421-431.

Maisanaba, S., Pichardo, S., Jorda-Beneyto, M., Aucejo, S., Camean, A. M. and Jos, A. 2019. Cytotoxicity and mutagenicity studies on migration extracts from nanocomposites with potential use in food packaging. Food and Chemical Toxicology 66: 366-372.

Malgurski, I., Levic, S., Nesic, A., Mitric, M., Pavlovic, V. B. and Dimitrijevic-Brankovic, S. 2017. Mineralized agar-based nanocomposite films: Potential food packaging materials with antimicrobial properties. Carbohydrate Polymers 175: 55-62.

Martinez-Sanz, M., Martinez-Abad, A. and Lopez-Rubio, A. 2019. Cost-efficient bio-based food packaging films from unpurified agar-based extracts. Food Packaging and Shelf Life 21: 1-9.

Mosman, T. 1983. Rapid colourimetric assay for cellular growth and survival: Application to proliferation and cytotoxicity assays. Journal of Immunological Methods 65(1-2): 55-63.

Noshad, M., Behbahani, B. A., Jooyandeh, H., Rahmati-Joneidabad, M., Kaykha, M. E. H. and Sheikhjan, M. D. 2021. Utilisation of plant major seed mucilage containing *Citrus limon* essential oil as edible coating to improve shelf-life of buffalo meat under refrigeration conditions. Food Science and Nutrition 9(3): 1625-1639.

Omerovic, N., Djisalov, M., Zivojevic, K., Mladenovic, M., Vunduk, J., Milenkovic, I., ... and Vidic, J. 2021. Antimicrobial nanoparticles and biodegradable polymer composites for active food packaging applications. Comprehensive Reviews in Food Science 20: 2428-2454.

Rhim, J. W., Wang, L. F. and Hong, S. I. 2013. Preparation and characterization of agar/silver nanoparticles composite films with antimicrobial activity. Food Hydrocolloids 33(2): 327-335.

Rhim, J. W., Wang, L. F., Lee, Y. and Hong, S. I. 2014. Preparation and characterization of bio-nanocomposite films of agar and silver nanoparticles: Laser ablation method. Carbohydrate Polymers 103: 456-465.

Roopan, S. M., Rohit, Madhumitha, G., Rahuman, A., Kamaraj, C., Bharathi, A. and Surendra, T. V. 2013. Low-cost and eco-friendly phyto-synthesis of silver nanoparticles using *Cocos nucifera* coir extract and its larvicidal activity. Industrial Crops and Products 43(1): 631-635.

Roy, S. and Rhim, J. W. 2019a. Agar-based antioxidant composite films incorporated with melanin. Food Hydrocolloids 94: 391-398.

Roy, S. and Rhim, J. W. 2019b. Melanin-mediated synthesis of copper oxide nanoparticles and preparation of functional agar/CuO nanocomposite films. Journal of Nanomaterials 2019: 1-10.

Roy, S., Rhim, J. W. and Jaiswal, L. 2019. Bioactive agar-based functional composite film incorporated with copper sulphate nanoparticles. Food Hydrocolloid 93: 156-166.

Sarwar, M. S., Niazi, M. B. K., Jahan, Z., Ahmad, T. and Hussain, A. 2018. Preparation and characterization of PVA/nanocellulose/Ag nanocomposite films for antimicrobial food packaging. Carbohydrate Polymers 184: 453-464.

Shankar, S. and Rhim, J. W. 2015. Amino acid mediated synthesis of silver nanoparticles and preparation of anti-microbial agar/silver nanoparticles composite films. Carbohydrate Polymers 130: 353-363.

Shankar, S. and Rhim, J. W. 2017. Preparation and characterization of agar/lignin/silver nanoparticles composite films with ultraviolet light barrier and antibacterial properties. Food Hydrocolloids 71: 76-84.

Shankar, S., Reddy, J. P. and Rhim, J. W. 2015a. Effect of lignin on water vapour barrier, mechanical and structural properties of

agar/lignin composite films. International Journal of Biological Macromolecules 81: 267-273.

Shankar, S., Teng, X. N., Li, G. and Rhim, J. W. 2015b. Preparation, characterization and antimicrobial activity of gelatin/ZnO nanocomposite films. Food Hydrocolloids 45: 264-271.

Shukla, M. K., Singh, R. P., Reddy, C. R. K. and Jha, B. 2012. Synthesis and characterization of agar-based silver nanoparticles and nanocomposite film with antibacterial applications. Bioresource Technology 107: 295-300.

Sureshjani, M. H., Yazdi, F. T., Mortazavi, S. A., Behbahani, B. A. and Shahidi, F. 2014. Antimicrobial effects of *Kelussia odoratissima* extracts against food borne and food spoilage bacteria *in vitro*. Archives of Advances in Biosciences 5(2): 115-120.

Taherimehr, M., YousefniaPasha, H., Tabatabaeekoloor, R. and Pesaranhajiabbas, E. 2021. Trends and challenges of biopolymer-based nanocomposites in food packaging. Comprehensive Reviews in Food Science and Food Safety 20(6): 5321-5344.